Morphological and mechanical properties of styrene butadiene rubber/nano copper nanocomposites

CrossMark

Maryam Hadizadeh Harandi [a], Fakhrodin Alimoradi [b], Gholamhussein Rowshan [c], Morteza Faghihi [a], Maryam Keivani [d,*], Mohamadreza Abadyan [e]

[a] Department of Chemical and Petroleum Engineering, Sharif University of Technology, Tehran, Iran
[b] Engineering Group, Chaloos Branch, Islamic Azad University, Chaloos, Iran
[c] Shahid Rajaeei Campus, Farhangian University, Shiraz, Iran
[d] Shahrekord University of Medical Sciences, Shahrekord, Iran
[e] Shahrekord Branch, Islamic Azad University, Shahrekord, Iran

A B S T R A C T

In this research, rubber based nanocomposites with presence of nanoparticle has been studied. Styrene butadiene rubber (SBR)/nanocopper (NC) composites were prepared using two-roll mill method. Transmission electron microscope (TEM) and scanning electron microscope (SEM) images showed proper dispersion of NC in the SBR matrix without substantial agglomeration of nanoparticles. To evaluate the curing properties of nanocomposite samples, swelling and cure rheometric tests were conducted. Moreover, the rheological studies were carried out over a range of shear rates. The effect of NC particles was examined on the thermal behavior of the SBR using thermal gravimetric analysis (TGA). Furthermore, tensile tests were employed to investigate the capability of nanoparticles to enhance mechanical behavior of the compounds. The results showed enhancement in tensile properties with incorporation of NC to SBR matrix. Moreover, addition of NC increased shear viscosity and curing time of SBR composites.

© 2016 The Authors. Published by Elsevier B.V. This is an open access article under the CC BY-NC-ND license (http://creativecommons.org/licenses/by-nc-nd/4.0/).

Introduction

In recent years, polymer nanocomposites have become the center of interest due to their appropriate properties. The use of nanomaterials in polymers is dramatically increased in recent years. The presence of nanofillers in polymer matrix results in improvement of mechanical [1–4], thermal [5,6], electrical [7,8] and rheological properties [9] of polymers. Among polymeric materials, rubbers are famous for their easy processing, crack resistance and high flexibility. With regard to these advantages, researchers have widely studied the preparation and performance of rubber nanocomposites [10,11]. Styrene butadiene rubber (SBR) is one of the synthetic rubbers that can be used as commercial matrix for rubber nanocomposites fabrication. Moreover, some researchers have focused on preparation and characterization of ternary SBR blends. SBR is a non-polar rubber and has good mechanical properties. Great demands of SBR motivates researchers to investigate on their nanocomposites [12–19].

Recently, copper/polymer composites are considered as promising materials due to their enhanced characteristics [20–23]. In this research, nanocopper (NC) particles are used to improve the mechanical and physical properties of SBR for the first time. A two-roll mill method is employed for mixing ingredients in SBR. This mixing method is attractive for commercial and industrial applications [24,25]. To the best of author's knowledge, the characteristics of SBR/NC nanocomposites have not been systematically addressed in the literature. Therefore, the influence of NC on curing behavior, swelling characteristics, rheology, thermal degradation, tensile performance and tear strength of SBR is explored.

Experimental

Materials

Styrene butadiene rubber (SBR 1502) as the matrix was supplied from Bandar Imam Petrochemical Co. (Iran). The density and the styrene content of SBR were 0.98 g/cm^3 and 23%, respectively. The curing system consisted of sulfur (S), zinc oxide (ZnO), stearic acid were supplied from Iran Petrochemical Co. (Iran). Tetramethyl thiuram disulphide (TMTD) and mercaptobenzothiazole disulphide (MBTS) were used as accelerator agents. Nanocopper was supplied from US Research Nanomaterials, Inc. with

* Corresponding author.
  E-mail address: maryam.keivani@yahoo.com (M. Keivani).

average particle size (APS) of 70 nm and specific surface area 6–8 m^2/g. The shape of NC particles was spherical and their density and purity were 8.9 g/cm^3 and 99.9% respectively. Industrial grades of toluene and acetone were used as solvents in extraction and swelling experiments.

Preparation of nanocomposites

A laboratory scale two-roll mill was used for blending the compounds. First, SBR was masticated for 3 min, then NC particles were added to SBR (at 2, 4 and 6 parts per hundred rubber (PHR)) and mixed for additional 10 min. Next, the curing agents (see Table 1 which summarizes the compositions) were added to the compound. The compounds were then mixed for another 10 min to achieve appropriate dispersion of the ingredients in the rubbery matrix. Afterwards, the compositions were cured for 60 min at 150 °C in compression molding process. The cure time was selected slightly higher than t_{95} (time to 95% cure) to ensure complete curing (100% cure) of the compounds. The value of t_{95} was determined by measuring the increase of the torque values of the none-vulcanized rubber compounds at 150 °C. After curing, test samples were cut from the obtained sheets.

Observation techniques

Dispersion of nanoparticles in the matrix was evaluated using transmission electron microscopy. The apparatus was Philips CM-200 TEM used at accelerating voltage of 200 kV. Ultra-thin section of samples was cut with OmU3 ultramicrotom (Reichert, Austria).

The fractured surface of tensile test sample was analyzed by scanning electron microscope (LEO, 1455VP, UK). The fractured surfaces were coated by a thin gold layer and SEM images were taken from the coated surfaces.

Characterization techniques

The cure characteristics of the compounds were measured via oscillating disk rheometer (ODR GT7070-S2, GOTECH, Taiwan) operated at 150 °C at a 1° arc and a frequency of 1.66 Hz based on ASTM D5289. The scorch time (t_s) and curing time (t_{95}) were obtained from torque difference. The cure rate index (CRI) was extracted from rheometric data via the following relation:

$$CRI = \frac{100}{t_{95} - t_s} \tag{1}$$

Swelling ratio of samples was determined by placing a piece of sample in toluene for 48 h. at room temperature. Regarding to size of the samples (1 cm × 1 cm with thickness of 2 mm), this time (48 h) is adequate for complete solvent diffusion into the samples. The swelling ratio was calculated with the following equation:

$$Swelling\ Ratio = \frac{x - y}{y} \tag{2}$$

where x and y are the weights of the sample after and before swelling, respectively. For calculating the average molecular weight between two crosslinks, M$_c$, Flory-Rehner relation was used as:

$$M_C = \frac{\rho_r V_S \left(\frac{v_r}{2} - v_r^{1/3}\right)}{\ln(1 - v_r) + v_r + \chi\, v_r^2} \tag{3}$$

where M$_c$ is the average molecular weight between two crosslinks, ρ_r is the density of rubber, V_S is the molar volume of solvent (V_S = 106.3 cm^3/mol for toluene), χ is the polymer-solvent interaction parameter (0.378 for SBR-toluene [26]) and v_r is the volume fraction of the rubber in swollen rubber (measured from the swelling experiment).

Melt flow behavior of compounds was investigated using capillary rheometer CEAST 1000 (Italy), with capillary die diameter (d) of 1 mm and length (l) of 40 mm. The rheological test was carried out at 150 °C over a range of shear rates i.e. 10–1000 s^{-1}. The apparent viscosity (η) was measured as the ratio of shear stress (τ) to shear rate ($\dot{\gamma}$). The shear stress was measured as $\tau = (\Delta P \times d)/4l$ and shear rate was calculated by $\dot{\gamma} = 32Q/(\pi d^3)$, where ΔP and Q are pressure drop and flow rate of compound, respectively.

Thermogravimetric analysis was conducted from room temperature to 500 °C at the heating rate 20 °C/min using Perkin-Elmer Diamond TG/DTA thermal analyzer. The analysis was carried out at a nitrogen atmosphere to prevent the oxidation of the samples. From the TGA results, temperature at 5 and 50% mass degradation (T_5, T_{50}) and temperature at maximum rate of mass loss (T_{max}) were obtained.

Tensile characteristics of compounds were measured using Hounsfield H10Ks testing machine at crosshead speed of 50 mm/min. Test samples were cut from vulcanized sheets of SBR compounds. For each compound at least five mechanical tests were performed.

Results and discussion

Morphology

Due to the high surface energy, nanoparticles incline to form agglomerates [27], hence, achieving good dispersion and distribution of nanofiller in matrix is still a critical issue in nanoparticle/rubber composites. Low and high magnification TEM images of SN6 sample are presented in Fig. 1a and b, respectively. As seen, most nanoparticles have been uniformly dispersed in the SBR matrix. However, some agglomerations can be seen in these images which consist of several NC particles that formed aggregates with size of 100–250 nm. Tendency of nanoparticles to form agglomerates in rubber matrix has been reported by some researchers [28,29].

Similar trend can be observed by SEM images (Fig. 1c and d) from fractured surfaces of SN6 sample. As seen, homogenous dispersion and distribution of NC particles are shown through the SBR matrix (Fig. 1c). It seems that NC particles have good interaction with SBR and there are no clear detachment of particles. Moreover, some separated NC particles is evidently observed in Fig. 1d which indicates proper de-agglomeration of nanoparticles in the polymer. Overall, one can conclude that NC particles are rather well dispersed and distributed in the rubber matrix. It implies that

Table 1
Formulations of compounds (all in PHR).

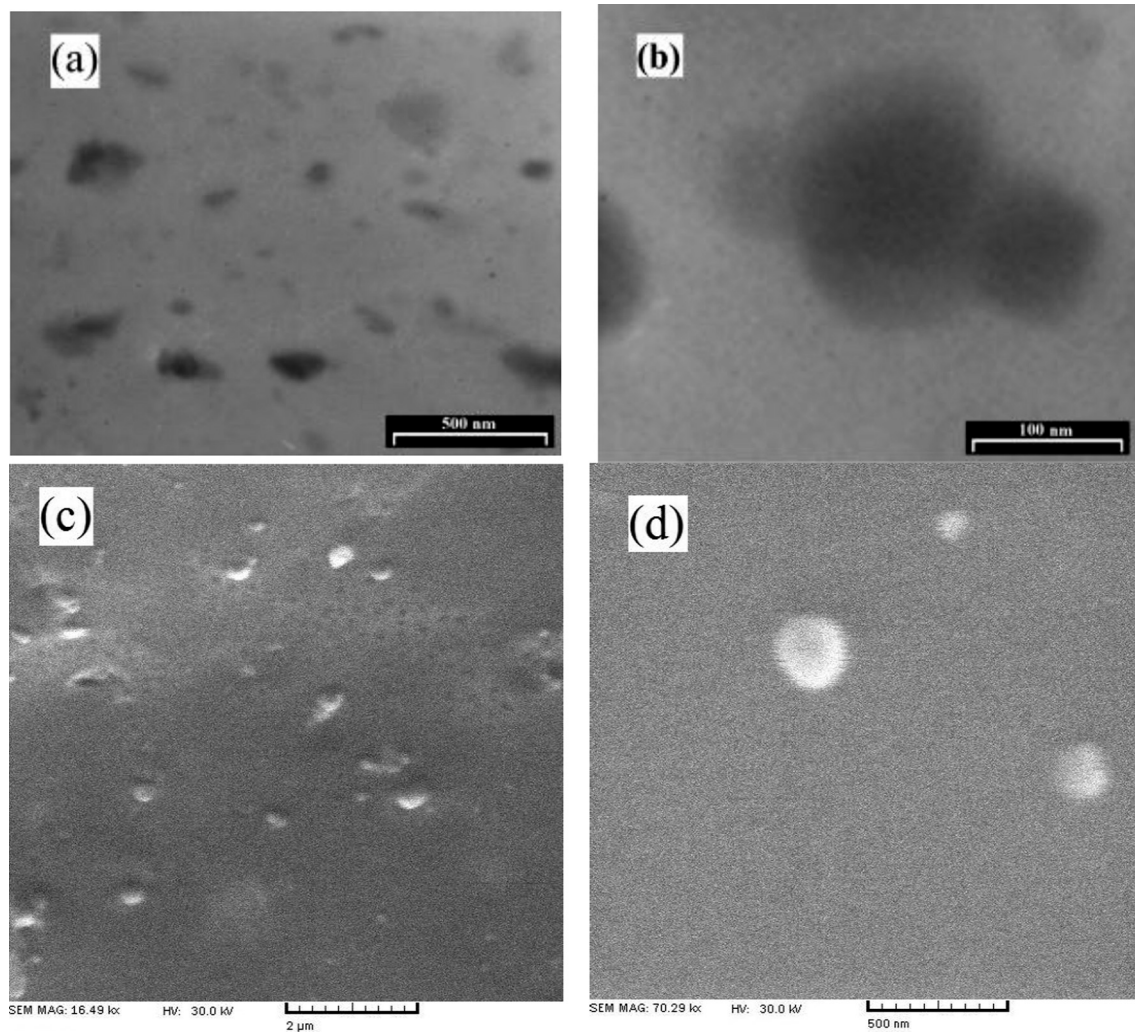| Sample	SBR	NC	Sulfur	ZnO	Stearic acid	MBTS	TMTD
S	100	0	3	5	1.5	1	0.2
SN2	100	2	3	5	1.5	1	0.2
SN4	100	4	3	5	1.5	1	0.2
SN6	100	6	3	5	1.5	1	0.2

Fig. 1. TEM images of SC6 sample at (a) low and (b) high magnifications and SEM images of fractured surface of SC6 at (c) low and (d) high magnifications.

Table 2
Rheometric cure results of SBR/NC nanocomposites.

Compound	t_S (Sec.)	t_{95} (Sec.)	CRI (s^{-1})	T_{min} (N.m)	T_{max} (N.m)
S	436	4160	2.69×10^{-2}	0.91	4.18
SN2	465	4785	2.31×10^{-2}	0.97	3.93
SN4	516	5294	2.09×10^{-2}	1.09	3.68
SN6	541	5966	1.84×10^{-2}	1.18	3.71

using two-roll mill method can be considered as proper tool for preparation of SBR/NC composites.

Cure characteristics

To investigate the vulcanization behavior of the SBR/NC nanocomposite samples, rheometric tests were conducted as summarized in Table 2. The vulcanization behavior of rubber nanocomposites can be expressed in terms of cure characteristics i.e. scorch time (t_S), cure time (t_{95}), minimum torque (T_{min}) and maximum torque (T_{max}) values.

As seen in Table 2, scorch time of neat SBR is 436 s. With increasing the NC content, scorch and cure times of SBR compounds are increased. This leads to decrease in cure rate index (CRI) which implies that NC particles slow down the cure reaction of SBR matrix. Previous researches have reported that nanofillers such as clay may facilitate the vulcanization reaction hence decrease the scorch and cure times of rubber compounds as compared with the unfilled rubber [30]. However, the present study shows that NC increases these parameters for SBR compounds. Increasing effect of nanoparticles on rubber scorch and cure times is frequently attributed to the partial adsorption of curing agents on the surface of nanoparticles [30].

Moreover, T_{min} of SBR is increased with increasing NC content. Addition of 6 PHR NC to SBR leads to about 30% increase in measured torque. The increase in T_{min} values can be interpreted via the increase in the viscosity of the compounds due to the presence of rigid copper particles. However, T_{max} of the SBR decreases with addition of nanocopper filler. As maximum torque is related to the crosslinking density of rubber [30], it might be concluded that NC decreases the crosslinking density of SBR. This issue is evaluated in the next section via swelling test.

Swelling behavior

Swelling ratio of SBR/NC nanocomposites have been presented in Fig. 2. Swelling ratio of neat SBR (S) is about 2.37. With addition of 2 PHR NC to SBR, swelling ratio is increased to 2.52 that shows 6% increase in comparison with neat SBR. No further change in the swelling ratio is observed beyond 2 PHR filler content.

The average molecular weight between two cross links (M_c) has been calculated from swelling test and the obtained values are illustrated in Fig. 3. As seen, addition of NC to SBR increases the M_c values of the matrix. For SN6 sample (with 6 PHR NC content), M_c is 4900 g/mol which is 26% higher than that of neat SBR (3900 g/mol).

Increase in M_c is equivalent to decrease in crosslinking density (ν) [31]. Fig. 4 shows the variation of crosslinking density of compounds versus NC content. The crosslink density, υ, is determined from the average molecular weight between two cross links using the following relation:

$$\upsilon = \frac{\rho_r}{M_C} \tag{4}$$

With increase in NC content from 0 to 6 PHR, the crosslinking density of SBR decreases from 0.00027 to 0.00021 mol/cm^3. Decrease in the crosslinking density with increase in NC content (Fig. 4) is in agreement with the decrease in maximum torque of samples that observed in cure rheometric test (see Table 2). Previous researchers hypothesized that decrease in crosslinking density due to addition of nanofillers might probably be the result of adsorption of some curing ingredients on the surface of the nanofiller [30].

Rheological properties

The shear viscosity versus shear rate of SBR/NC nanocomposites was measured and the obtained results have been shown in Fig. 5. The viscosity values continuously decrease with increase in shear rate, presents a shear thinning effect in all samples. Shear thinning trend that obeying the Power-Law model [32], may be originated from polymer chains orientation under shear forces [33,34]. Note that the addition of NC does not change the shear thinning behavior of the compounds, but it influences the extent of viscosity at a given shear rate. Fig. 5 reveals that with addition of NC particles, the shear viscosity of SBR matrix have been increased especially
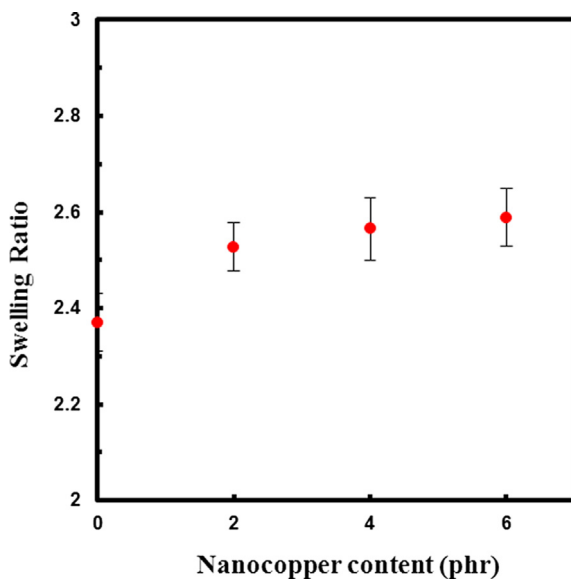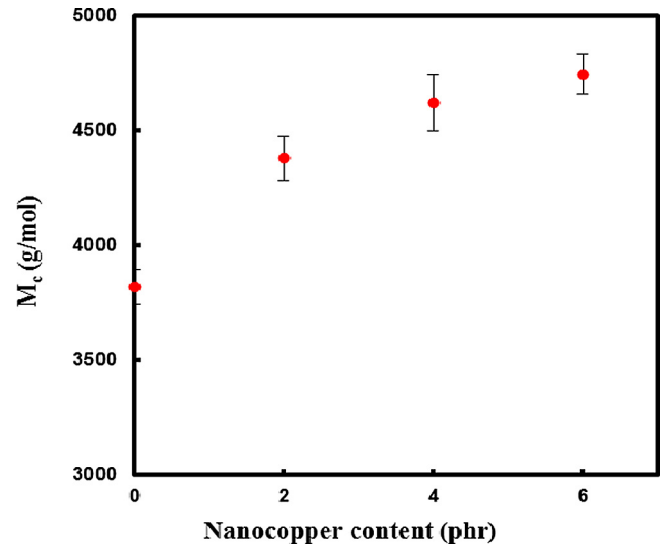
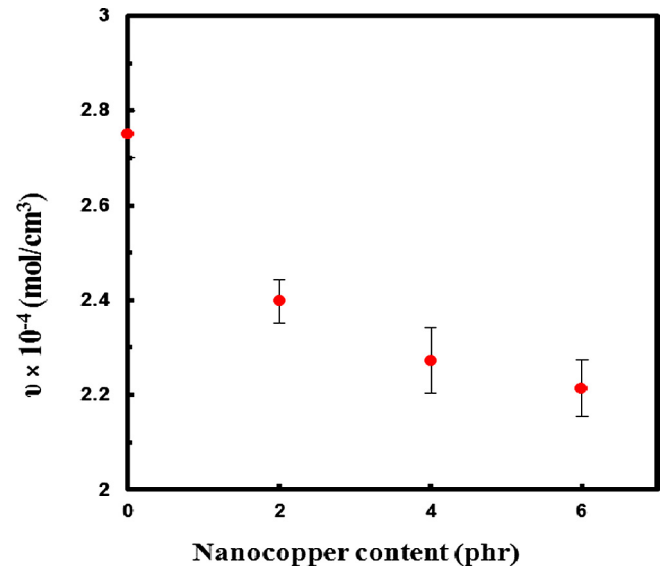**Fig. 3.** M_c versus nanocopper content.

Fig. 4. Crosslinking density versus nanocopper content.

in low shear rates. This is similar to the finding of previous researchers who reported increase in shear viscosity with addition of layered silicate [35].

For better understanding, the special shear viscosity values at distinct shear rate (121.6 s^{-1}) are listed in Table 3. The shear viscosity at this shear rate for unmodified sample (S) is 4.48 kPa-s. With addition of NC to SBR, shear viscosity is gradually increased. The highest increase in shear viscosity is observed for SN6 sample in which 11% increase in shear viscosity was happened. This increase in shear viscosity can be attributed to good SBR/NC interaction and proper dispersion of NC in SBR matrix [33] that provides hindrance against deformation and flow of polymer matrix.

Thermal degradation characteristics

Fig. 6 shows degradation thermograms of the SBR/NC samples that represents the variation of mass loss versus temperature. This figure shows that the mass loss of samples are negligible for temperatures lower than 250 °C. While by increasing the temperature
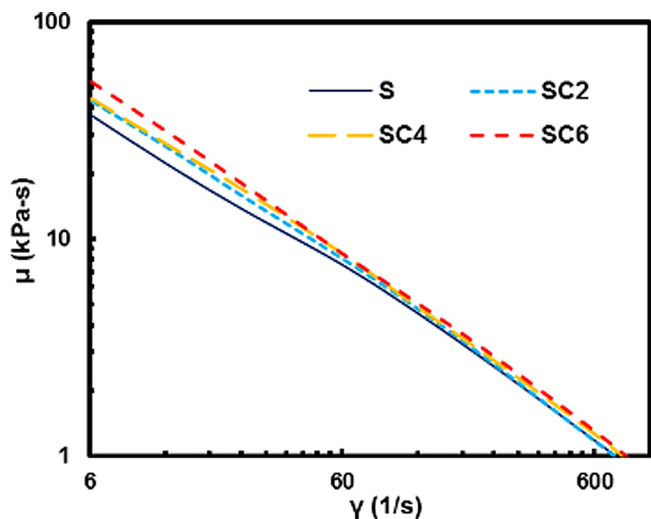
Fig. 2. Swelling ratio of SBR/NC nanocomposites.

Fig. 5. Shear viscosity as a function of shear rate at 150 °C for gum SBR and SBR/NC compounds.

Table 3
Shear viscosity at 121.6 s^{-1} of shear rate for SBR/NC nanocomposites.

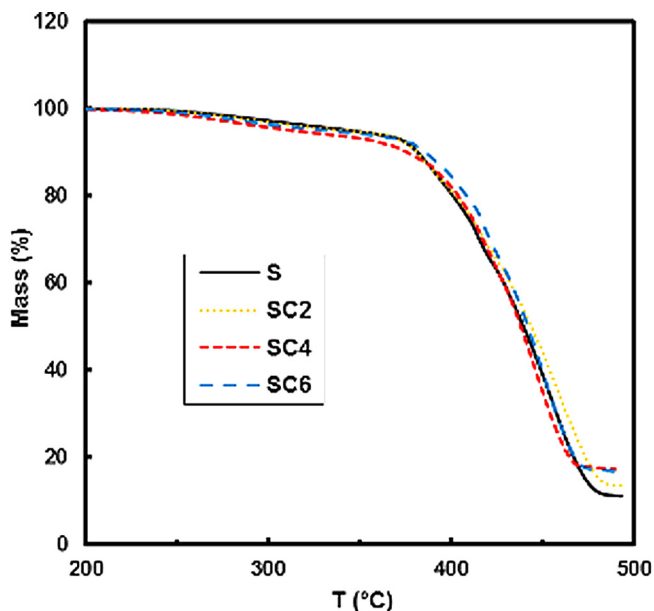| Compound	Shear viscosity at 121.6 s^{-1} (kPa-s)
S	4.48
SN2	4.68
SN4	4.77
SN6	4.98

Fig. 6. TGA weight loss of SBR/NC samples versus temperature.

beyond this value, polymer degradation becomes substantially important.

Thermal characteristics of SBR/NC nanocomposites are listed in Table 4. In this table, T_5 and T_{50} reveal the temperatures correspond to the onset of polymer degradation (5% mass loss) and the substantial polymer degradation (50% mass loss), respectively. Moreover, with calculating differential thermogravimetric of curves, T_{max} is calculated which reveals the temperature at maximum rate of losing mass.

Table 4
TGA results for SBR/NC nanocomposites.

Compound	T_5 (°C)	T_{50} (°C)	T_{max} (°C)
S	343	440	452
SN2	340	436	449
SN4	338	437	451
SN6	331	440	452

As seen, T_5 of unmodified rubber (S) is 343 °C. With addition of NC particles to SBR, T_5 values are gradually decreased. The highest decrease in T_5 is observed for SN6 with 6 PHR NC. The behavior of polymeric nanocomposites at the onset of thermal degradation can be viewed in terms of the ability of chain scission and free radical diffusion in the polymer matrix [36,37]. Lee et al. [37] have mentioned that there is a direct relation between suppression of chain mobility and elevating the thermal stability of nanocomposites. In this work, increasing the NC content reduces the crosslinking density of the matrix (Fig. 4). Decrease in crosslinking density and concomitant increase in mobility of the polymer chains accelerates the polymer degradation. This can be the reason of decrease in T_5 with increase in filler content.

The T_{50} is also another indicator of thermal resistance of polymers. At this weight loss (50%), most of the polymer chains are degraded by oxidation or chain scission and the material does not attain its initial properties. Table 4 shows that addition of NC particles causes a slight decrease in T_{50} of the SBR/Cu nanocomposites. Similar trend is observed for T_{max} values. This trend is different from that reported for NC/LDPE system where copper nanoparticles increased the thermal stability of low density polyethylene compounds [23]. The obtain results show that incorporation of NC has a deteriorating effect on the thermal stability of SBR. This could be attributed to reduction in crosslinking density as well as the high thermal conductivity of the copper nanoparticles.

While compared with the non-metal nanoparticles (such as nanoclay), the incorporation of the NC has different influence on thermal stability of SBR nanocomposites. This difference may be due to the fact that the activity of the metal nanoparticles is much higher than that of the non-metal nanoparticles. The higher the activity of the nanoparticles, the higher the surface energy of the nanoparticles is [23]. Therefore, the thermal degradation of the NC/SBR requires less energy than that of the SBR/non-metal nanocomposites, resulting in different thermal stability of the materials.

Tensile properties

Tensile characteristics i.e. tensile strength and modulus for each sample were measured and the average values are illustrated in Fig. 7. The values of tensile properties of neat SBR are in agreement with those available in the literature [15]. The tensile strength (Fig. 7a) and secant modulus (at 50% strain) (Fig. 7b) of SBR samples increases with increasing the NC content. About 81% improvement in tensile strength and 55% increase in secant modulus of SBR are obtained by addition of 6 PHR NC filler (SN6). The improvement in tensile properties implies direct evidence of the good polymer-filler interactions [38]. This increase in mechanical characteristics corresponds to proper dispersion of NC in SBR which enhances the interaction and load transfer between matrix and NC particles. This proper interaction and dispersion of NC with SBR matrix was observed in rheology results (see Fig. 5 and Table 3). The reinforcing effect of well-dispersed fillers on a rubber matrix can be explained via the increase in stiffness of the soft rubber matrix due to the rigidity/strength of particulate fillers [39].
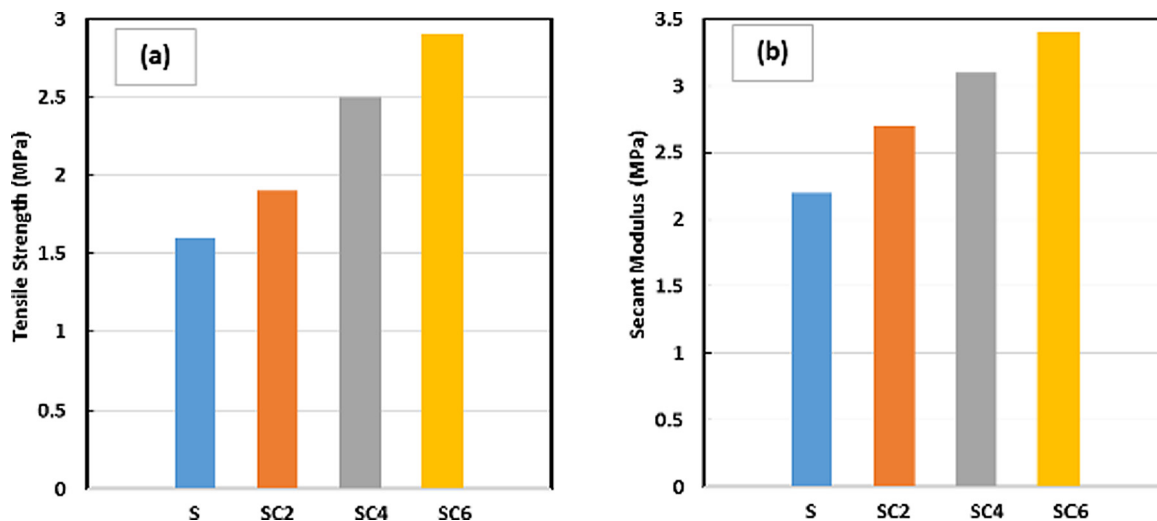
Fig. 7. Mechanical properties of SBR/NC nanocomposites: (a) tensile strength and (b) secant modulus.

Conclusions

Fabrication of SBR/NC nanocomposites was conducted using two-roll mill method. TEM images showed good dispersion and uniform distribution of NC particles. Results revealed that:

- Addition of NC to SBR slightly increased the swelling ratio while decreased the crosslinking density of the compounds.
- Addition of NC increased scorch and curing times of SBR. The minimum torque is increased due to viscosity increasing caused by the rigid particles. However, the maximum torque is decreased due to the crosslinking density reduction.
- Rheological measurements revealed that the shear viscosity of SBR matrix is increased with increasing the NC content (especially in low shear rates) while is decreased with increasing the shear rate (shear thinning effect).
- Incorporation of NC had a deteriorating effect on the thermal stability of SBR. It can be attributed to reduction in matrix crosslinking density besides the higher thermal resistance of NC.
- Tensile strength and secant modulus of nanocomposites are increased as the result of good dispersion and interaction of NC with SBR matrix and high rigidity/strength of the fillers.

Acknowledgement

References

[1] Wu CL, Zhang MQ, Rong MZ, Lehmann B, Friedrich K. Functionalization of polypropylene by solid phase graft polymerization and its effect on the mechanical properties of silica nanocomposites. Plast Rubber Compos Macromol Eng 2011;32(10):445–50.

[2] Kovarova L, Kalendova A, Simonik J, Malac J, Weiss Z, Gerard JF. Effect of melt processing conditions on mechanical properties of polyvinylchloride/organoclay nanocomposites. Plast Rubber Compos Macromol Eng 2004;33(7):287–94.

[3] Salehi Vaziri H, Abadyan M, Nouri M, Amiri Omaraei I, Sadredini Z, Ebrahimnia M. Investigation of the fracture mechanism and mechanical properties of polystyrene/silica nanocomposite in various silica contents. J Mater Sci 2011;46:5628–38.

[4] Jumahat A, Soutis C, Jones FR, Hodzic A. Compressive behaviour of nanoclay modified aerospace grade epoxy polymer. Plast Rubber Compos Macromol Eng 2012;41(6):225–32.

[5] He XJ, Wang LJ, Xie XL, Zhang K. Investigation of thermal property and flame retardancy of ABS/montmorillonite nanocomposites. Plast Rubber Compos Macromol Eng 2010;39(2):54–60.

[6] Lai X, Zeng X, Li H, Liao F, Yin C, Zhang H. Synergistic effect of phosphorus-containing montmorillonite with intumescent flame retardant in polypropylene. J Macromol Sci, Phys 2012;51(6):1186–98.

[7] Jiang J, Zhang D, Zhang Y, Zhang K, Wu G. Influences of carbon nanotube networking on the conductive, crystallization, and thermal expansion behaviors of PA610-based nanocomposites. J Macromol Sci, Phys 2013;52(7):910–23.

[8] Rashmi SH, Raizada A, Madhu GM, Kittur AA, Suresh R, Sudhina HK. Influence of zinc oxide nanoparticles on structural and electrical properties of polyvinyl alcohol films. Plast Rubber Compos Macromol Eng 2015;44(1):33–9.

[9] Salehi Vaziri H, Amiri Omaraei I, Abadyan M, Mortezaei M, Yousefi N. Thermophysical and rheological behavior of polystyrene/silica nanocomposites: investigation of nanoparticle content. Mater Des 2011;32:4537–42.

[10] Cadambi RM, Ghassemieh E. Influence of nanoclays on mechanical and barrier properties of hydrogenated acrylonitrile butadiene rubber nanocomposites. Plast Rubber Compos Macromol Eng 2011;40(6–7):283–8.

[11] Sadeghi Ghari H, Shakouri Z, Shirazi MMA. Evaluation of microstructure of natural rubber/nano-calcium carbonate nanocomposites by solvent transport properties. Plast Rubber Compos Macromol Eng 2014;43(6):177–86.

[12] Ghasemi I, Karrabi M, Ghorieshy MHR. Investigation into stress–strain behaviour of organoclay SBR composite using different constitutive models. Plast Rubber Compos Macromol Eng 2008;37(7):305–10.

[13] Girun N, Ahmadun FR, Rashid SA, Atieh MA. Multi-wall carbon nanotubes/styrene butadiene rubber (SBR) nanocomposite. Fullerenes, Nanotubes, Carbon Nanostruct 2007;15:207–14.

[14] Gallo E, Schartel B, Schmaucks G, von der Ehe K, Böhning M. Effect of well dispersed amorphous silicon dioxide in flame retarded styrene butadiene rubber. Plast Rubber Compos Macromol Eng 2013;42(1):34–42.

[15] Sadhu S, Bhowmick AK. Preparation and properties of styrene–butadiene rubber based nanocomposites: the influence of the structural and processing parameters. J Appl Polym Sci 2004;92:698–709.

[16] Le Cam JB, Huneau B, Verron E. Failure analysis of carbon black filled styrene butadiene rubber under fatigue loading conditions. Plast Rubber Compos Macromol Eng 2014;43(6):187–91.

[17] Zhang H, Wang Y, Wu Y, Zhang L, Yang J. Study on flammability of montmorillonite/styrene-butadiene rubber (SBR) nanocomposites. J Appl Polym Sci 2005;97:844–9.

[18] Bhattacharya M, Biswas S, Bhowmick AK. Permeation characteristics and modeling of barrier properties of multifunctional rubber nanocomposites. Polymer 2011;52:1562–76.

[19] Kim WS, Paik HJ, Bae JW, Kim W. Effect of polyethylene glycol on the properties of styrene-butadiene rubber/organoclay nanocomposites filled with silica and carbon black. J Appl Polym Sci 2011;122(3):1766–77.

[20] Lekka M, Koumoulis D, Kouloumbi N, Bonora PL. Mechanical and anticorrosive properties of copper matrix micro- and nano-composite coatings. Electrochim Acta 2009;54(9):2540–6.

[21] Akamatsu K, Ikeda S, Nawafune H, Deki S. Surface modification-based synthesis and microstructural tuning of nanocomposite layers: monodispersed copper nanoparticles in polyimide resins. Chem Mater 2003;15:2488–91.

[22] Cioffi N, Torsi L, Ditaranto N, Tantillo G, Ghibelli L, Sabbatini L, Bleve-Zacheo T, D'Alessio M, Giorgio Zambonin P, Traversa E. Copper nanoparticle/polymer composites with antifungal and bacteriostatic properties. Chem Mater 2005;17(21):5255–62.

[23] Xia X, Cai S, Xie C. Preparation, structure and thermal stability of Cu/LDPE nanocomposites. Mater Chem Phys 2006;95:122–9.

[24] Wang YQ, Wu YP, Zhang HF, Zhang LQ, Wang B, Wang ZF. Free volume of montmorillonite/styrene-butadiene rubber nanocomposites estimated by positron annihilation lifetime spectroscopy. Macromol Rapid Commun 2004;25(23):1973–8.

[25] Guo B, Lei Y, Chen F, Liu X, Du M, Jia D. Styrene–butadiene rubber/halloysite nanotubes nanocomposites modified by methacrylic acid. Appl Surf. Sci 2008;255:2715–22.

[26] George SC, Ninan KN, Thomas S. Effect of degree of crosslinking on swelling and mechanical behaviour of conventionally vulcanised styrene-butadiene rubber membranes. Polym Compos 1999;7(5):343–53.

[27] Tang E, Cheng G, Ma X, Pang X, Zhao Q. Surface modification of zinc oxide nanoparticle by PMAA and its dispersion in aqueous system. Appl Surf Sci 2006;252:5227–32.

[28] Hwang WG, Wei KH. Mechanical, thermal, and barrier properties of NBR/organosilicate nanocomposites. Polym Eng Sci 2004;44(11):2117–24.

[29] Abu Bakar NHH, Ismail J, Abu Bakar M. Synthesis and characterization of silver nanoparticles in natural rubber. Mater Chem Phys 2007;104:276–83.

[30] Mai YW, Yu ZZ. Polymer nanocomposites. 1st ed. England: Woodhead Publishing Limited and CRC Press LLC; 2006. p. 318.

[31] Kim J, Kim WS, Lee DH, Kim W, Bae JW. Effect of nano zinc oxide on the cure characteristics and mechanical properties of the silica-filled natural rubber/butadiene rubber compounds. J Appl Polym Sci 2010;117:1535–43.

[32] Sadhu S, Bhowmick AK. Unique rheological behavior of rubber based nanocomposites. J Polym Sci, Part B: Polym Phys 2005;43:1854–64.

[33] Lim SK, Kim JW, Chin IJ, Choi HJ. Rheological properties of a new rubbery nanocomposite: polyepichlorohydrin/organoclay nanocomposites. J Appl Polym Sci 2002;86:3735–9.

[34] Zhong Y, Kee DD. Morphology and properties of layered silicate-polyethylene nanocomposite blown films. Polym Eng Sci 2005;45:469–77.

[35] Stephen R, Alex R, Cherian T, Varghese S, Joseph K, Thomas S. Rheological behavior of nanocomposites of natural rubber and carboxylated styrene butadiene rubber latices and their blends. J Appl Polym Sci 2006;101 (4):2355–62.

[36] Pandey JK, Reddy KR, Kumar AP, Singh RP. An overview on the degradability of polymer nanocomposites. Polym Degrad Stab 2005;88:234–50.

[37] Lee JY, Liao Y, Nagahata R, Horiuchi S. Effect of metal nanoparticles on thermal stabilization of polymer/metal nanocomposites prepared by a one-step dry process. Polymer 2006;47:4979–7970.

[38] Thomas Paul K, Pabi SK, Chakraborty KK, Nando GB. Nanostructured fly ash–styrene butadiene rubber hybrid nanocomposites. Polym Compos 2009;30 (11):1647–56.

[39] Ahmed S, Jones FR. A review of particulate reinforcement theories for polymer composites. J Mater Sci 1990;25:4933–42.